

QUARTZ CRYSTAL MICROBALANCE / HEAT CONDUCTION CALORIMETRY STUDY OF SOLVENT SORPTION IN THIN C₆₀ AND C₆₀-PIPERAZINE FILMS

J. Tian and A. L. Smith*

Department of Chemistry, Drexel University, Philadelphia, PA 19104, USA

* Author to whom correspondence should be addressed

The quartz crystal microbalance / heat conduction calorimeter (QCM / HCC) developed in our laboratory has been used to investigate the sorption of water and organic solvents in thin films of C₆₀ and C₆₀-piperazine monoadduct. Films of 1-5 μ thickness and 2 cm² area were spray-deposited on the quartz crystal microbalance surface, and were then exposed in QCM/HCC to various partial pressures of solvent vapor in a N₂ carrier gas at 25°C. Solvents included water, 1,3-dichlorobenzene, carbon tetrachloride, and methylene chloride. Simultaneous measurement of mass uptake and heat dissipation in the film at 25°C as a function of solvent partial pressure gives new information on the thermodynamics and kinetics of solvate formation in C₆₀ and C₆₀-piperazine, complementing prior studies of solvate formation with differential scanning calorimetry. QCM/HCC studies also show if the solvate formation at 25°C is irreversible or if the solvate is easily decomposed at low solvent vapor pressures.

INTRODUCTION

One important property of molecular solids such as C₆₀ and its derivatives is its interaction with solvents. The review by Korobov and Smith (1) indicates that C₆₀ readily forms solvates at room temperature with a number of solvents, and previous work by Tian et al (2) indicate that C₆₀-piperazine also forms solvates. Of course, direct measures of the solute-solvent interaction are the solubility of the solid in the solvent and the decomposition temperature and enthalpy of the solvate, but it is also possible to probe solvent/C₆₀ interaction by doing vapor sorption experiments. We have developed a new gravimetric/calorimetric experimental method in our laboratory that permits such vapor sorption studies: quartz crystal microbalance/heat conduction calorimetry, or QCM/HCC. In this paper, we discuss the interaction of thin solid films of C₆₀ and C₆₀-piperazine monoadduct with a series of gases whose liquid phases can be used to dissolve these solids. We measure sorption isotherms and sorption enthalpies of the gases in the films, as well as measures of the rate of equilibration of the gas and the solid.

Overview of Instrumentation

Quartz Microbalance / Microcalorimetry is a new gravimetric / calorimetric method. In our laboratory the instrumentation has the acronym QCM/HCC (Quartz Crystal Microbalance / Heat Conduction Calorimetry) (3). A quartz crystal microbalance is mounted on brass electrodes and in thermal contact with thermopiles. A sample is coated on the QCM and mounted on the microbalance's electrodes. A gas flow stream with variable vapor composition of solvent is applied to the sample film. Mass and thermal signals are recorded and to precision of ± 10 ng and ± 50 nW respectively. The experiment is carried in an isothermal water bath.

Variable Solvent Vapor Flow

Solvent vapor pressure is varied in a stepwise change. The solvent vapor flow is controlled by two mass flow controllers. A total flow of 40 cc/min of nitrogen gas is combined through the use of two mass flow controllers labeled MFC-1 and MFC-2. The carrier gas stream of MFC-2 travels through a glass solvent bubbler containing pure solvent. The outlet of the gas stream is 100% saturated with the solvent vapor at the given temperature (25°C in these experiments).

The outlet flow from of MFC-2 combines with the pure dry flow of MFC-1 at a T-joint for a total gas flow of 40 cc/min. By varying the flow rates of MFC-1 and MFC-2 a desirable vapor pressure is obtained.

Using a Labview program the instrument is controlled to apply stepwise changes in vapor activity at a desired rate. In this particular experiment we applied solvent vapor at 15% increments for 6 steps between the maximum vapor activity of 90% and the minimum activity of 0.

The Quartz Crystal Microbalance

Quartz crystal exhibits the converse piezoelectric effect -- an applied voltage generates a mechanical deformation. This property of quartz is used to detect trace mass loadings on the QCM and has been reviewed by Ward and Buttry (4) and by Grate, Martin, and White (5). A small uniform mass load on the surface of the quartz will reduce the oscillating resonant frequency of the quartz. The change of frequency can be detected and the relationship between the frequency shift and mass load is described by the Saurebrey Equation [1](6).

$$\frac{\Delta f}{f_0} = \frac{-\Delta e}{e_0} = \frac{-2f_0\Delta m}{A\sqrt{\rho\mu}} \quad [1]$$

Here Δe is the change in the original thickness e_0 , A is the piezoelectrically active area, and ρ and μ are the density and shear modulus of quartz. By measuring the frequency change it is possible to calculate the mass of material deposited on the crystal, and this is the principle of the quartz crystal microbalance (QCM). The application of the QCM in chemistry for sensitive detection of gases adsorbed on solid absorbing surfaces has been reviewed by Alder and McCallum (7) and again by McCallum (8).

The Heat Flow Sensor

In heat flow calorimetry, the heat flow from the sample to a heat sink is measured as a function of time. The sensor in a heat conduction calorimeter is a Peltier effect thermoelectric module, or thermopile. The thermal power P detected by a thermopile is given by the Tian equation [2](9).

$$P = \frac{1}{S} \left[U + \tau \left(\frac{dU}{dt} \right) \right] \quad [2]$$

Where P is the thermal power (W), S is the thermopile sensitivity (V/W), U is the thermopile voltage (V), and τ is the time constant of the calorimeter. At a steady state, $U=S \cdot P$, the output voltage is proportional to the thermal power dissipated on the thermopile surface. The time constant τ of a heat conduction calorimeter is C/G , where C is the reaction vessel heat capacity and G is the thermal conductance of the thermopile. For our apparatus, $\tau=53$ seconds.

The voltage output of the thermopiles was amplified by a low noise nanovoltmeter and recorded. A thermal trace of thermal power vs. time is obtained. Integration of the thermal trace gives a heat trace vs. time plot.

EXPERIMENTAL

The Apparatus

Figure 1 shows a sketch of total assembly of the QCM/HCC instrumentation. Figure 2 shows a block diagram of the whole apparatus constructed at Drexel University. The mass sensors are 5MHz AT-cut QCM's (Maxtek, P/N 149211-1, model SC-501-1) with dimensions: 2.54 cm in diameter and 0.33 mm in thickness. The 160nm thick top and bottom gold electrodes on the QCM are vacuum-deposited onto a 15nm chromium

adhesion layer. The larger top electrode (12.9mm in diameter) is used as the active surface. However, the region of the quartz exposed to the rf electric field is limited to that directly beneath the smaller electrode (6.6mm in diameter) resulting in a mass sensitive area of approximately 0.32cm^2 (10). Both sample and reference quartz resonators are driven by rf oscillator circuits as described by Auge et al (11). The oscillation frequencies of the QCM's are measured individually with an HP 53131A frequency counter interfaced to a Macintosh computer through a GPIB interface.

Each QCM rests on two double horse-shoe shaped brass electrodes, which serve both to apply radio frequency power to the QCM and to conduct heat generated on the QCM surface to the top of the thermopile. The heat flow sensors are 1cm^2 FC 0.45-66-05 thermopiles (Melcor, Trenton NJ). Four thermocouple plates are used in the QCM/HCC. Two are connected in series to form one heat flow sensor on the reference side, and the same arrangement is used for the sample side. The differential signal of the sample and reference sides is amplified by EM Model N15 Nanovoltmeter and recorded on the same Macintosh computer with an A/D board under the control of Labview software (National Instruments, Inc.).

Film Preparation

C_{60} and C_{60} -piperazine samples were loaded on the quartz crystal resonators as thin films. The oscillating capillary nebulizer (OCN) (12) was used to deposit the thin films. OCN is a device that is able to deposit a uniform and thin film on a surface. A solution containing the sample to be deposited is injected into a fused silica capillary with a $50\text{ }\mu\text{m}$ i.d. This capillary is friction mounted inside another fused silica capillary, $250\text{ }\mu\text{m}$ i.d. Helium is then introduced into the larger capillary thus causing the inner capillary to oscillate. This oscillation causes the solution to be nebulized at the capillary tip.

RESULT AND DISCUSSION

Water Vapor Sorption Experiment on C_{60} -Piperazine

An experiment was carried out on a C_{60} -piperazine film with mass of $493\text{ }\mu\text{g}$ and thickness of $1.56\text{ }\mu$ (assuming the density of C_{60} -piperazine is 1.6 g/cm^3). Water vapor was applied to the film surface in stepwise changes of 16% vapor activity for a total of 6 steps (Figure 3). The actual water vapor activity applied to the sample is not at a sharp stepwise change as depicted by the mass flow controller voltage (Figure 4). The change of the water vapor activity is slower because it takes about 17 seconds for the gas flow to reach the film sample from mass flow controller. This time is negligible compared to the time the film is exposed to a particular vapor activity.

With an increased vapor activity the sample film absorbs solvent vapor, resulting in an increase of mass (Figure 5).

Associating with the mass change of the sample, heat was generated when absorption and desorption occurred. This heat change is shown as a peak on thermal signal trace (Figure 6). Exothermic signals (shown as upward peaks) during absorption are distinguishable from endothermic peaks (shown as downward peaks) during desorption. Integration of the thermal power signal trace with time yields a heat trace with respect to time (Figure 7).

Comparing the mass trace and thermal trace the shapes of the plots are correlated and the difference of signal level for each step can be determined. Using the difference of the heat value and mass value, the enthalpy of sorption is calculated at each step.

For this water vapor sorption experiment on C₆₀-piperazine film, the calculated enthalpy of sorption has an average value of 43 kJ/mole of water. This value is close to the enthalpy of evaporation of water at 25°C, 44 kJ/mole. One interpretation of this result is that the water is condensed into the free volume between C₆₀-piperazine molecules, and that C₆₀-piperazine / H₂O interactions are not as important as H₂O / H₂O interaction. The sorption isotherm plot of water gain versus relative humidity is shown (Figure 8).

Results for this water vapor sorption experiment on C₆₀-piperazine are similar to that of water vapor in polymers (12).

1,3-Dichlorobenzene Vapor Experiment on C₆₀-Piperazine Film

1,3-dichlorobenzene was selected for this experiment because it is a good solvent for C₆₀-piperazine. Solubility measurements were described in authors' previous ECS meeting proceeding (2). 1,3-dichlorobenzene vapor was applied in the same incremental steps as the water vapor (Figure 9).

On the mass trace, a curvature is seen for the increasing of mass upon each stepwise change (Figure 10). For each step the solvent does not reach equilibrium with the film before solvent vapor activity is changed. This shows that 1,3-dichlorobenzene sorption by C₆₀-piperazine film is a much slower process than water sorption, presumably because of the larger molecular size of the aromatic solvent.

The accompanying thermal trace was not recorded due to electronic difficulty.

Carbon tetrachloride Vapor Experiment on C₆₀ Film

For a 454 μg (1.44 μ thickness) C_{60} film, on the mass trace of this experiment there is mass gain and loss cycle associated with the changing applied vapor activity (Figure 11). However, the expected mass traces are much different from the “ideal” behavior of water vapor on C_{60} -piperazine film (Figure 12). Two major aspects are observed. First, the increase of mass at mass increasing steps is not equally distributed for each step. At the last mass gain step (vapor activity changed from 37.2% to 47.3%) the change of mass is more than 2 times greater than the previous step.

For the steps of decreasing mass there are about average mass losses for each step but the desorption solvent does not leave the film reversibly since the mass signal does not return to its baseline for each complete cycle. During this experiment two complete cycles were measured. The mass trace of the second cycle has a similar shape when compared with first cycle and again does not return to the original mass value upon desorption of the solvent.

We interpret this as incipient solvate formation of C_{60} and carbon tetrachloride. C_{60} forms solvates with many organic solvents (1). The formation of solvates take place when the solvent vapor activity reaches a certain level. The unusually large increase of mass at the highest solvent activity step suggests solvate formation takes place at this solvent vapor activity level.

For the given time of vapor exposure to the sample film, formation of the solvate does not reach equilibrium. In fact the mass change correspond to mole ratio of CCl_4 : C_{60} about 1 : 600. The reported CCl_4 / C_{60} solvate has a composition of $\text{C}_{60} \cdot 13\text{CCl}_4$ (1).

Besides the formation of a solvate between the solvent and sample film, there is also simple dissolution of solvent into the sample. Equal fraction mass loss when the solvent vapor activity was decreased support the suggestion of simple dissolution.

In this experiment the mass change at each step is at $\sim 0.1\mu\text{g}$ scale. This result shows the high sensitivity of the quartz crystal microbalance. However the change of mass is so low that the change of heat flow is too low to be resolved (Figure 13).

Methylene Chloride Vapor Experiment on C_{60} Film

For a 124 μg (0.393 μ thickness) C_{60} film, the solvent vapor activity of methylene chloride was change manually in this experiment. Activities were changed in increments at 25% for three steps (Figure 14). Similar to the carbon tetrachloride, there was a leap in mass trace occurring at the highest vapor activity of methylene chloride (Figure 15). When the solvent vapor activity decreased, each step shows the sample film released nearly equal amounts of solvent. That is similar to the observation of carbon tetrachloride experiment.

The integrated heat trace presents a change of total heat of on cycle of -1.2 mJ for a mass gain of 3.5 ug (figure 16), or calculated enthalpy of 24 kJ/mole for methylene chloride trapping into the film. From mass trace the mole ratio of CH₂Cl₂ : C₆₀ is 1 : 4. The composition of the known solvate is C₆₀·2CH₂Cl₂ (14). Thus, one cycle of vapor sorption and desorption is not long enough to convert the C₆₀ completely into solvate.

CONCLUSION

We have developed a new analytical instrumentation for micro scale gravimetric / calorimetric analysis. It has great advantage for solvent vapor sorption study on thin films. QCM / HCC is suitable for studying molecular crystal like C₆₀ and C₆₀-piperazine. It was found that water vapor sorption into C₆₀-piperazine film is primarily a physo-sorption. Aromatic solvent like 1,3-dichlorobenzene sorption into C₆₀-piperazine film is a slower process than water. Also observation of carbon tetrachloride and methylene chloride sorption into C₆₀ films match early study of solvate formation and confirm the stability of solvate at 25°C.

REFERENCES

1. Y. Marcus, A. L. Smith, M. V. Korobov, A. L. Mirakyan, N. V. Avramenko, and E. B. Stukalin, *J. Phys. Chem. B*, **105**, 2499 (2001).
2. J. Tian, D. Scheesley, A. L. Smith, E. Stukalin, A. Avramenko, and M. V. Korobov, in *Fullerenes for the New Millennium*, Kadish and Ruoff, Editors, p. 381, The Electrochemical Society Proceedings Series, Pennington, NJ (2001).
3. A. L. Smith, H. Shirazi, I. Wadso, in *Recent Advances in the Chemistry and Physics of Fullerenes and Related Materials*, Kadish and Ruoff, Editors, p. 576, The Electrochemical Society Proceedings Series, Pennington, NJ (1998).
4. M. D. Ward and D. A. Buttry, *Science*, **249**, 1000 (1990).
5. J. W. Grate, S. J. Martin, and R. M. White, *Analytical Chemistry*, **65**, 940A (1993).
6. G. Sauerbrey, *Z. Physik*, **155**, 206 (1959).
7. J. F. Alder, J. J. McCallum, *Analyst*, **108**, 1169 (1983).
8. J. J. McCallum, *Analyst*, **114**, 1173 (1989).
9. I. Wadsö, *Chem. Soc. Rev.*, **1997**, 79 (1997).
10. S. J. Marting, V. E. Grantstaff, and G. C. Frye, *Anal. Chem.*, **63**, 2272 (1991).
11. J. Auge, P. Hauptmann, J. Hartmann, S. Rosler, and R. Lucklum, *Sensors and Actuators B*, **24-25**, 43, (1995).
12. J. Perez, C. Petzold, M. A. Watkins, W. E. Vaughn, and H. Kenttamaa, *American Soc. of Mass Spec.*, **10**, 1105 (1999).
13. A. L. Smith and H. M. Shirazi, *J. Thermal Anal. and Calorimetry*, **59**, 171 (2000).
14. V. Krishnan, G. Moninot, D. Dubois, W. Kutner, and K. Kadish, *J. Electroanal. Chem.*, **356(1-2)**, 93, 107.

Figure 1. Overall Assembly of QCM/HCC Instrumentation

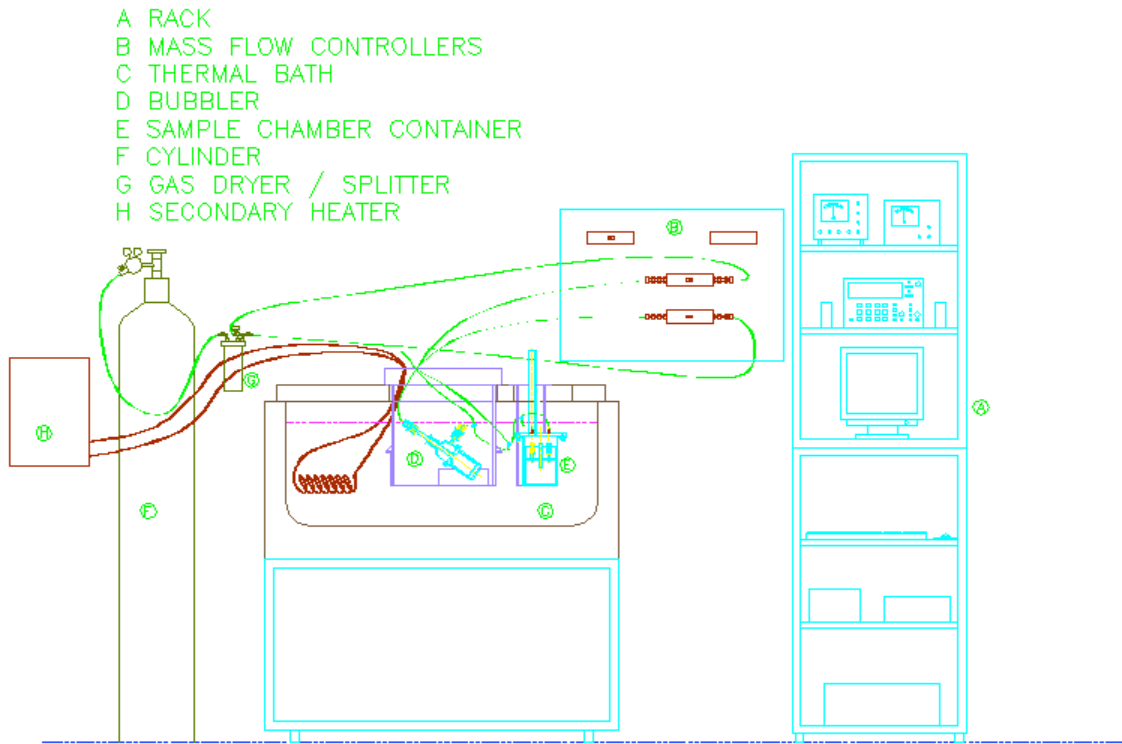


Figure 2. Block Diagram of Instrument

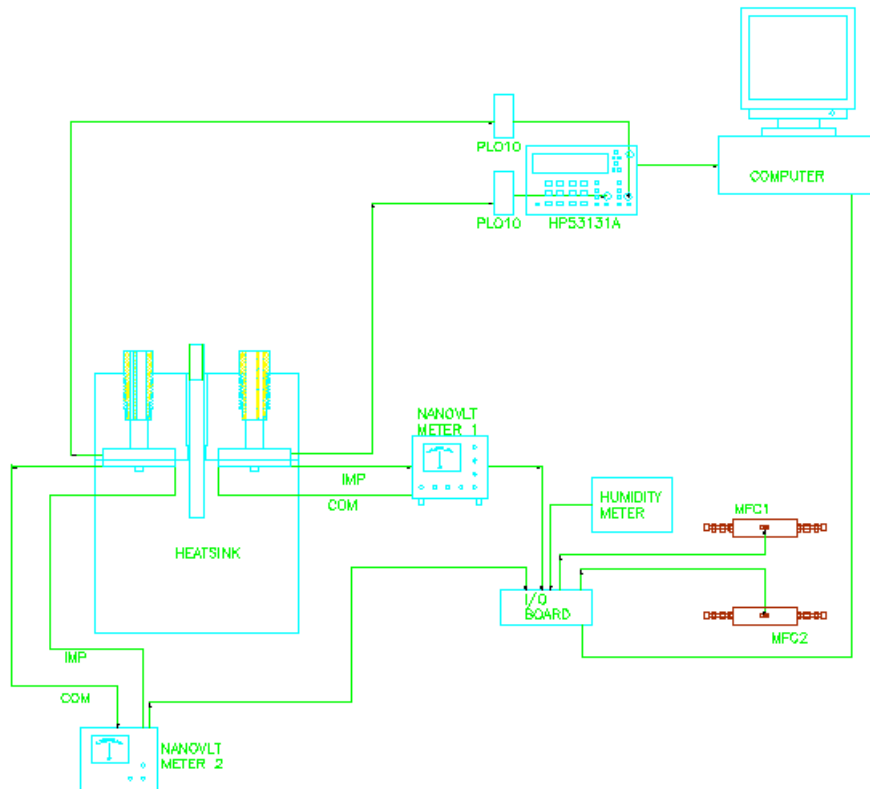


Figure 3.

**Relative Humidity Calculated from
Mass Flow Controller Response
Water Vapor on C60-Piperazine Film**

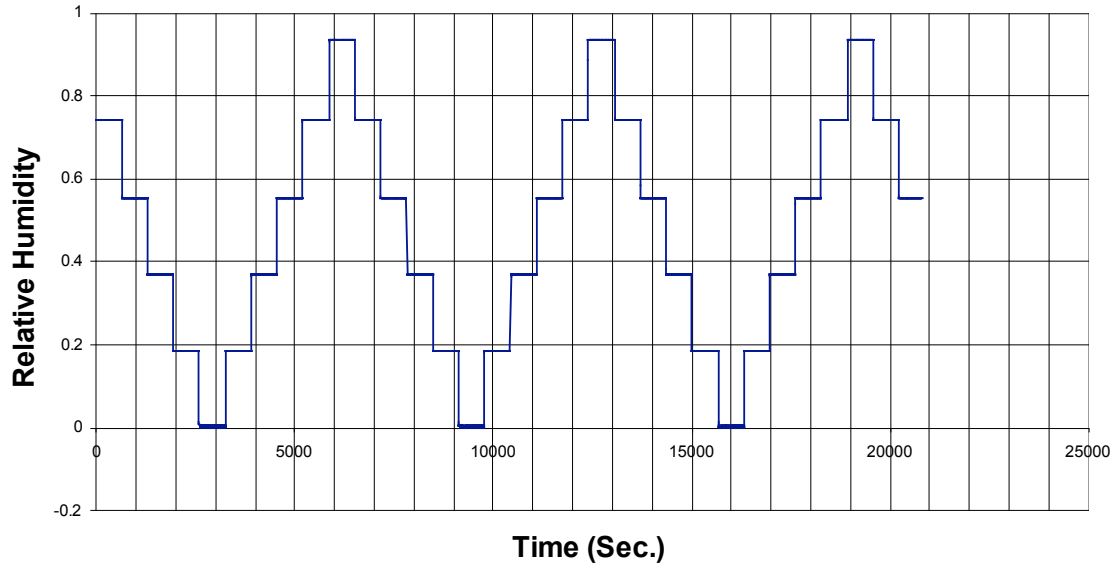


Figure 4.

**Detected Relative Humidity
Water Vapor on C60-piperazine film**

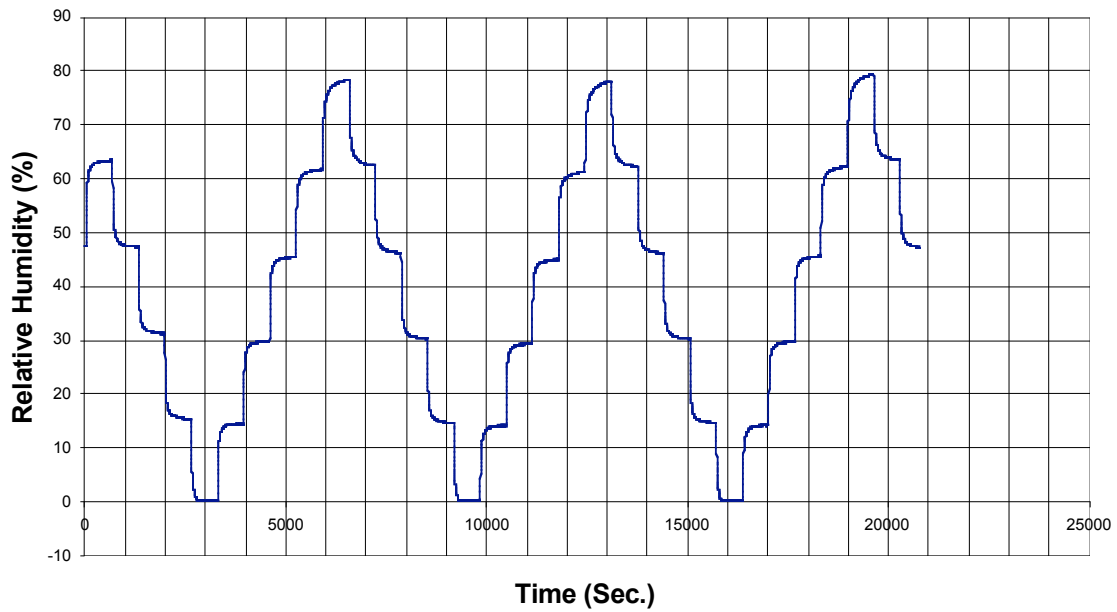


Figure 5.

**Mass Trace (Film Mass = 493 μ g)
Water Vapor on C60-Piperazine Film**

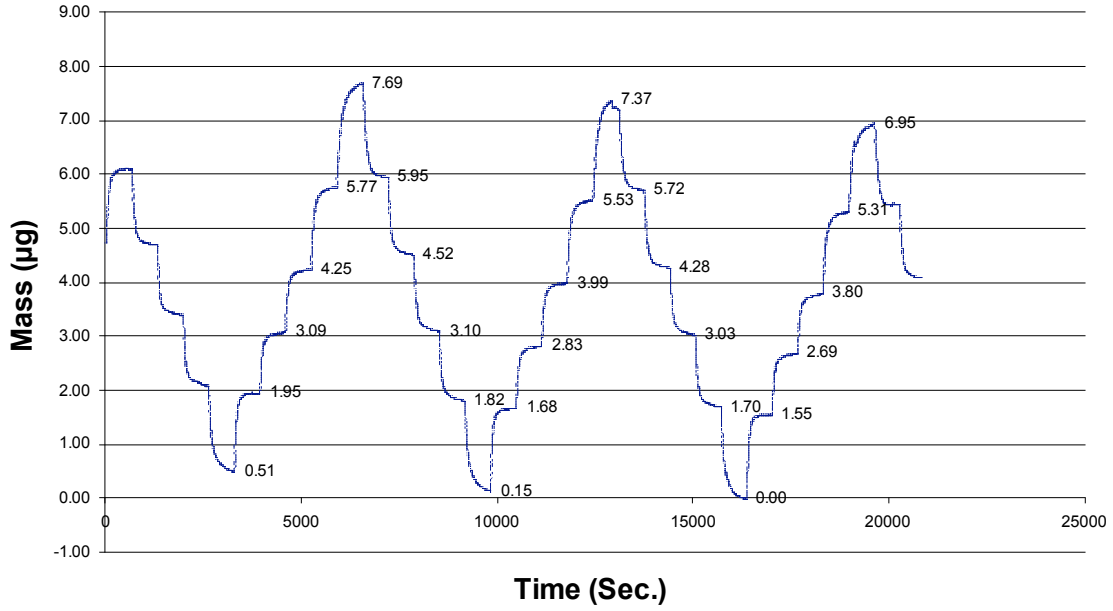


Figure 6.

**Thermal Trace
Water Vapor on C60-Piperazine Film**

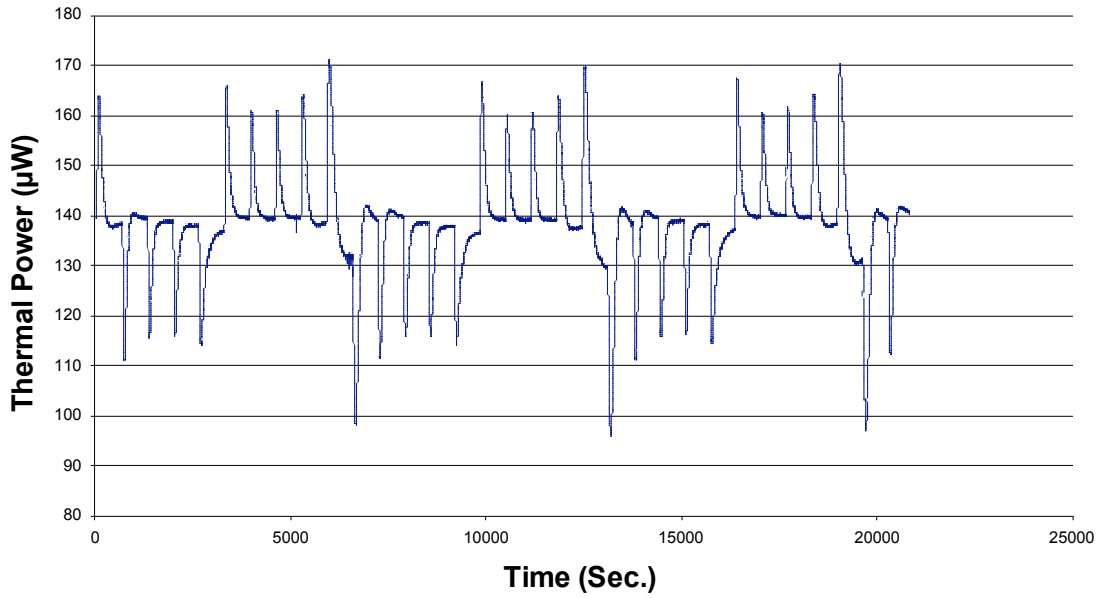


Figure 7.

Integrated Heat Trace Water Vapor on C60-Piperazine Film

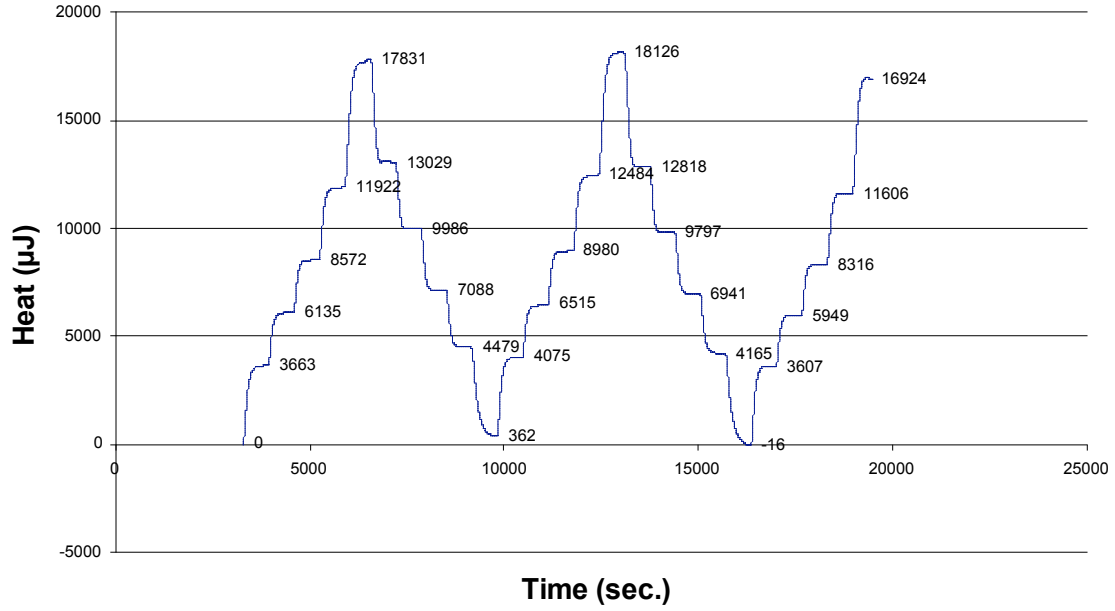


Figure 8.

Water Vapor on C60-Piperazine Film Sorption Isotherm Plot

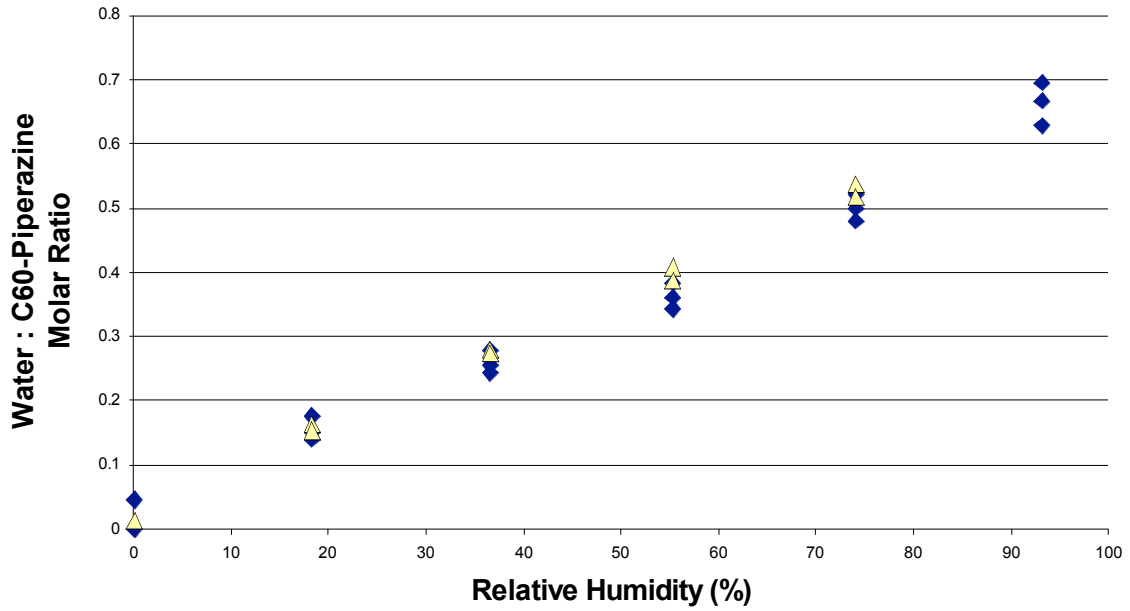


Figure 9.

**1,3-Dichlorobenzene on C60-Piperazine Film
Mass Flow Controller Response**

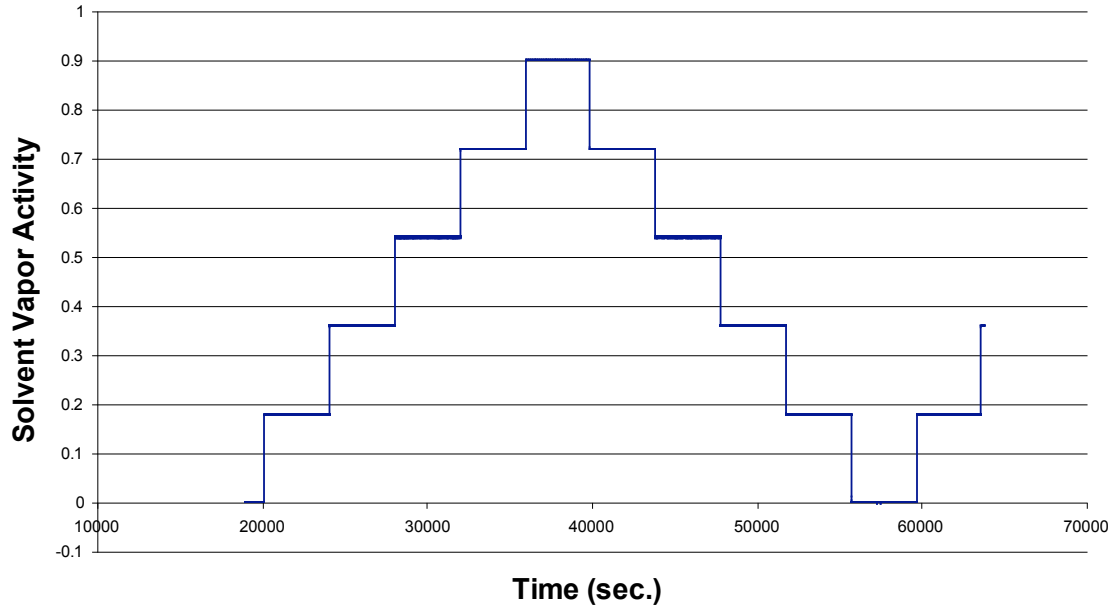


Figure 10.

**1,3-Dichlorobenzene Vapor on C60-Piperazine Film
Mass Trace**

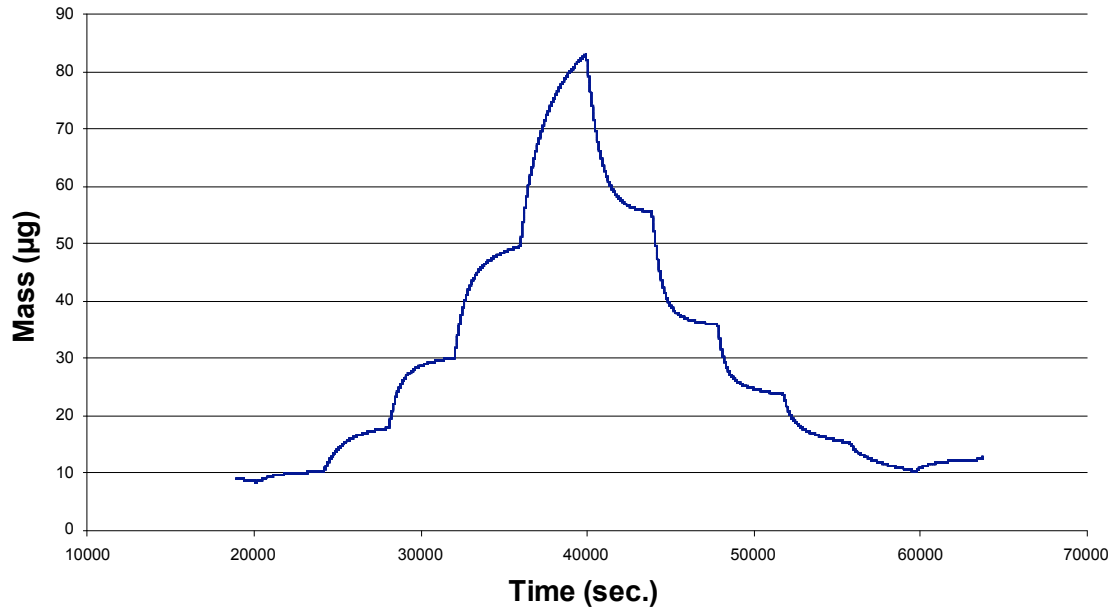


Figure 11.

**Carbon Tetrachloride on C60 Film
Mass Flow Controller Response**

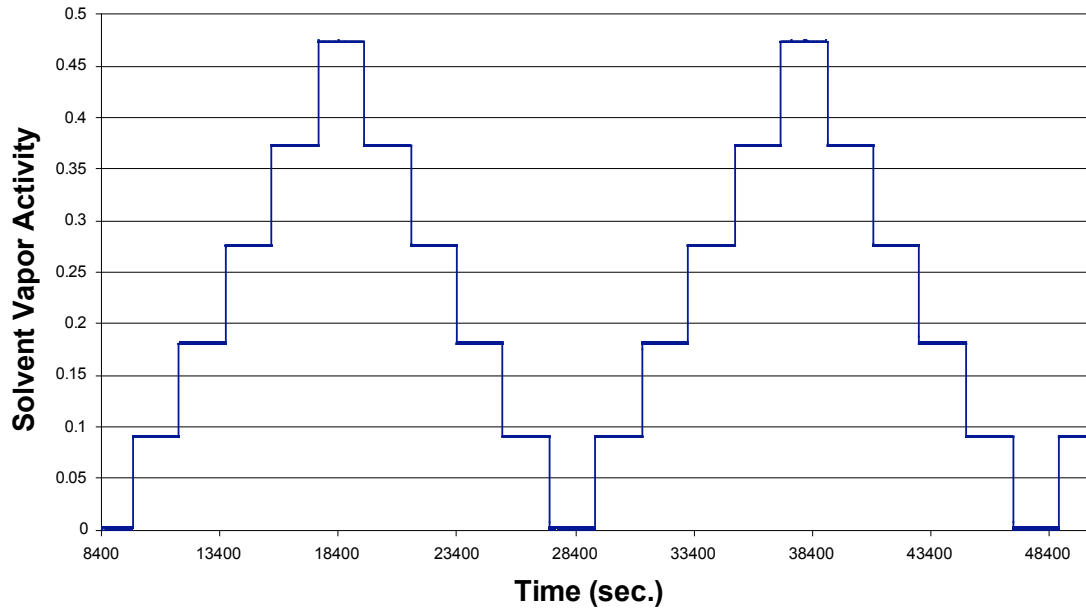


Figure 12.

**Carbon Tetrachloride on C60 Film
Mass Trace**

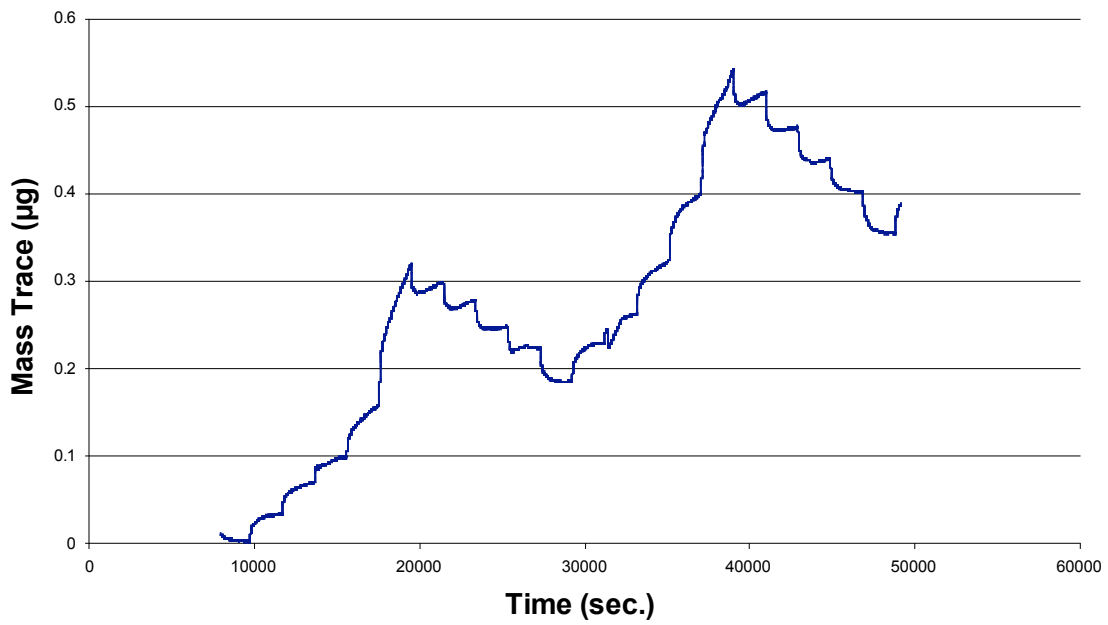


Figure 13.

**Carbon Tetrachloride on C60 Film
Thermal Trace**

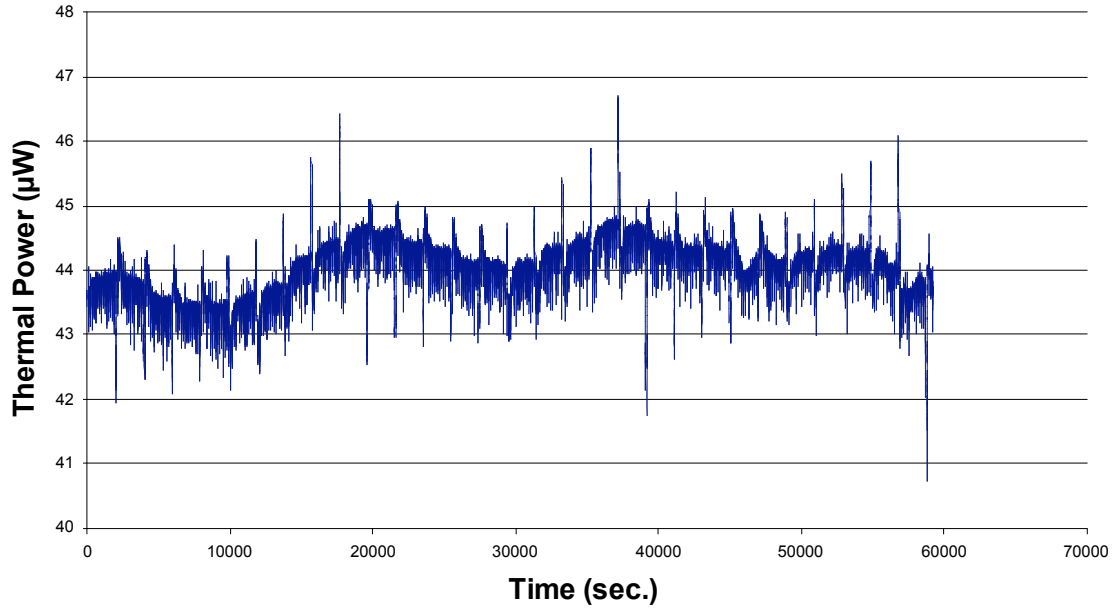


Figure 14.

**Methylene Chloride on C60 Film
Mass Flow Controller Response**

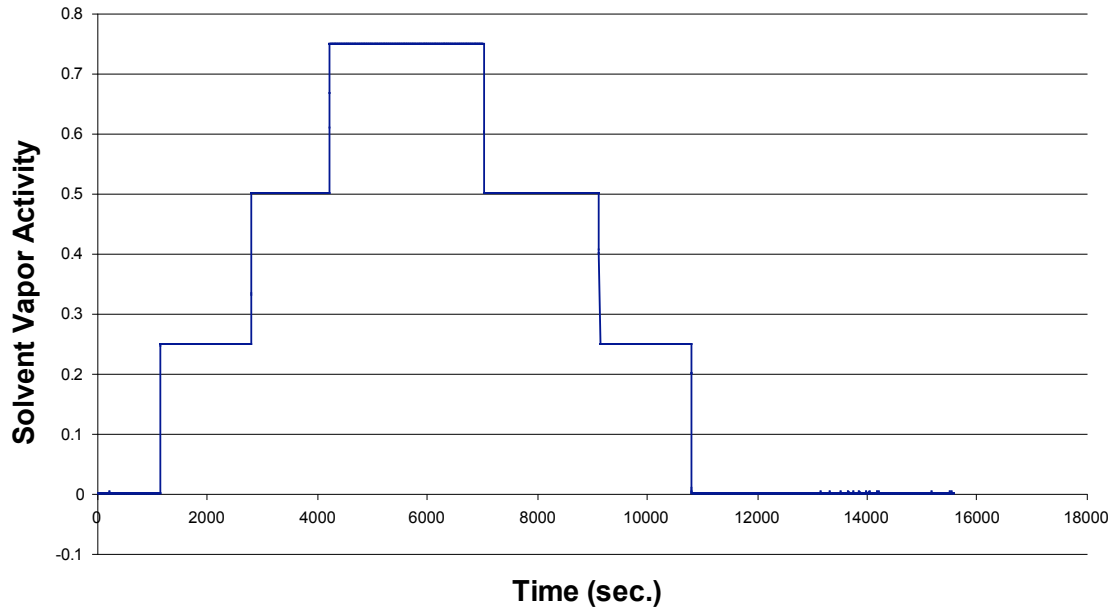


Figure 15.

Methylene Chloride on C60 Film Mass Trace

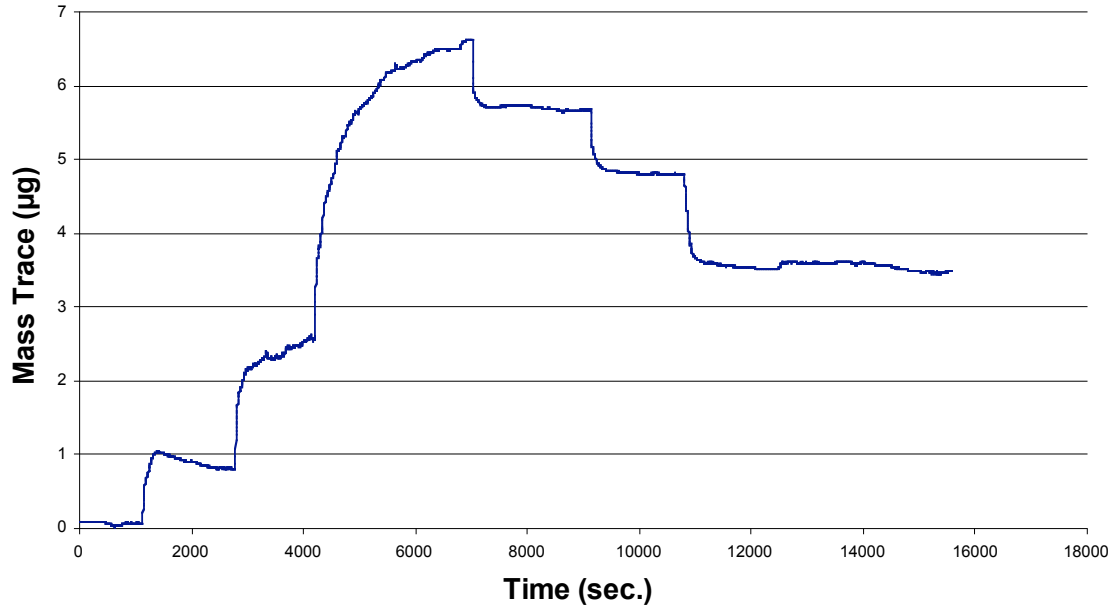


Figure 16.

Methylene Chloride on C60 Film Integrated Heat Trace

